

LITHIUM INTERCALATION IN PREFERENTIALLY ORIENTED LiCoO₂ FILMS

P.J. Bouwman, B.A. Boukamp, H.J.M. Bouwmeester, P.H.L. Notten[‡]

Laboratory of Inorganic Materials Science, Faculty of Chemical Technology & MESA+ Research Institute, University of Twente, PO Box 217, 7500 AE Enschede, the Netherlands. Contact: bouwman@nrl.navy.mil; <http://ims.ct.utwente.nl/>

[‡] Philips Research Laboratory, Professor Holstlaan 4, 5656 AA Eindhoven, Netherlands.

[‡] Eindhoven University of Technology, P.O. Box 513, 5600 MB Eindhoven, Netherlands.

Submicron films of LiCoO₂ have been deposited on silicon and stainless steel substrates using RF sputtering and Pulsed Laser Deposition (=PLD). Both types of film show preferred orientation. RF-films exhibit an *a*-axis orientation and have their Li diffusion plane oriented favourably, i.e. perpendicular to the surface, while PLD-films show a parallel, *c*-axis orientation. Electrochemical experiments indicate a strong dependence of the intercalation rate on the alignment of the host structure towards the electrolyte solution. Lithographic patterning enhances the inferior intercalation properties of the PLD-film on silicon, as does the utilisation of stainless steel substrates.

INTRODUCTION

Submicron LiCoO₂ films of stoichiometric composition have been prepared using various vacuum deposition techniques, in order to study the lithium intercalation mechanism of this popular electrode material in detail without the influence of additives.

The layered LiCoO₂ intercalation host can be derived from the rocksalt structure. The structure is rhombohedral (space group $R\bar{3}m$) with cobalt and lithium alternately occupying octahedral sites between adjacent close-packed oxygen planes. Approximately half of the lithium can reversibly be extracted and re-inserted electrochemically, before any structural degradation occurs. Diffusion of lithium proceeds within the lithium plane and is strictly two-dimensional.

In previous work it has been shown that stoichiometric LiCoO₂ can be deposited on silicon substrates with different preferential orientations (1). Films deposited with the Pulsed Laser Deposition (PLD) technique showed the (00 l) or *c*-axis orientation (*c*-film), while RF-sputtering produced a (110) or *a*-axis orientation (*a*-film) (Figure 1). Here, it is shown that the preferential orientation is related to the rate of deposition and not directly to the deposition technique. High LiCoO₂ film growth rates consistently produce *c*-films.

Due to the two-dimensional lithium diffusion planes, the preferential orientation of the LiCoO₂ films has a large influence on its electrochemical intercalation performance (2). The '*a*-films' are expected to have a superior intercalation rate, as their lithium diffusion plane is directed towards the electrolyte solution, contrary to the '*c*-films' which have

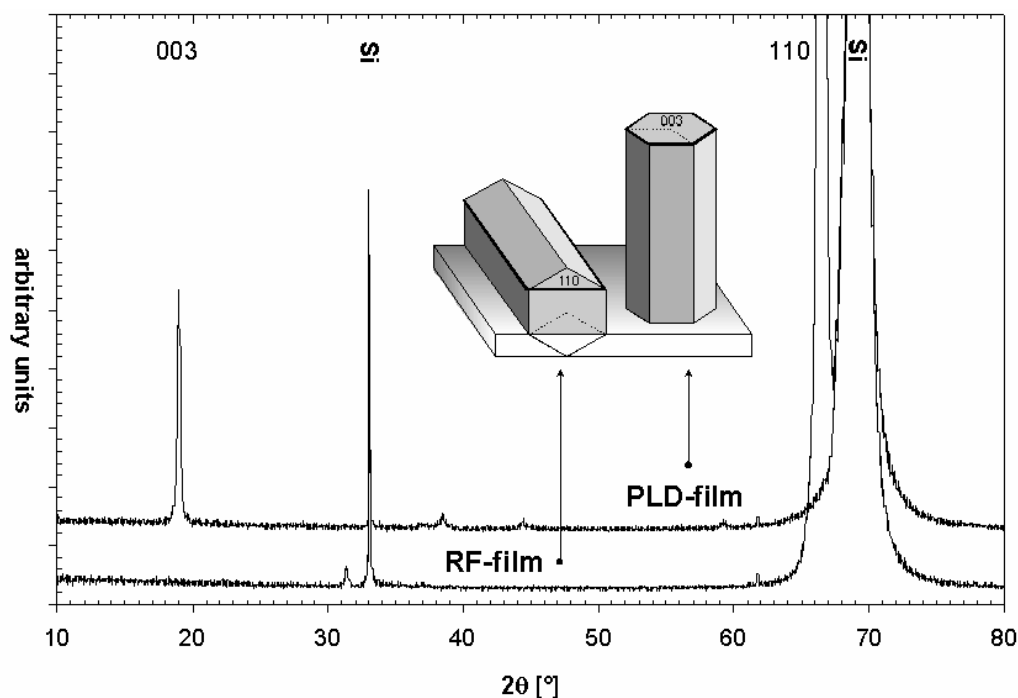


Figure 1: XRD spectra of a typical RF- and PLD-film, referred to as *a*-film and *c*-film respectively, after annealing at 600°C for 30 min (50 W RF-power). The inset shows the orientation of the LiCoO₂ unit cell toward the silicon substrate surface.

their diffusion plane oriented parallel with the electrolyte interface. In this paper measurement results are presented in which the electrochemical properties of typical '*a*-films' and '*c*-films' are characterised and compared to verify this hypothesis.

LiCoO₂ films on metallic substrates, while exhibiting *c*-axis orientation, are reported to show reasonable intercalation behaviour (3,4,5). The combination of cheap substrate materials and high-speed deposition methods appears as an attractive way of producing thin film electrodes. However, due to the random morphology, these are unsuitable for further study. Here, we present our attempts to modify our well-defined *c*-films on silicon substrates, to examine how the effect of its adverse preferential orientation can be counteracted. This information will benefit the understanding of the rate-limiting processes involved with the lithium (de-)intercalation. A full model description of the observed electrochemical behaviour will be presented in a future publication.

EXPERIMENTAL

Submicron LiCoO₂ films were prepared on silicon and stainless steel substrates with Pulsed Laser Deposition and RF-sputtering using stoichiometric LiCoO₂ targets. The silicon substrates (15 mm in diameter) were doped with phosphor to obtain n-type electrical conductivity. The metal substrate discs (15 mm in diameter) were stamped from

sheet metal and polished with diamond paste (1 μm). For the deposition parameters used with RF sputtering and PLD we refer to previously published work (1). Annealing was performed ex-situ in a constant gas flow of 30 $\text{ml}\cdot\text{min}^{-1}$ (standard temperature pressure (STP)) containing 90% O_2 / 10% N_2 to maintain the correct oxide stoichiometry. The standard annealing process was 30 min at 600°C using a ramp rate of 2°C·min⁻¹ (ex-situ).

The crystal structure of the submicron films was analysed with X-ray diffraction using $\text{CuK}\alpha$ at room temperature with a Philips PW 1800 diffractometer fitted with a rotating sample holder and an automatic divergence slit. Visualisation of the film surface morphology was performed using a JEOL JSM 5800 Scanning Electron Microscope.

Electrochemical experiments were conducted with a PGstat20 Autolab Potentiostat (ECO-Chemie) using an integrated Frequency Response Analyser. The electrochemical cell comprised three electrodes: a metallic lithium counter and reference electrode and the working electrode. Commercial battery grade liquid electrolyte (1 M LiClO_4 , EC:DEC 1:1, Merck) was used. The cells were maintained and operated inside a helium glove box.

In some *c*-films square islands of 0.1 mm^2 were bared at 0.1 mm spacing using standard lithographic techniques. These were etched with 5% HF solution leaving a gauze-like pattern in the LiCoO_2 film. Experiments with dry-etching are based on argon plasma milling, which enabled smaller mesh dimensions to be used (specified in text). One quarter of the active material was always removed in the process. These etched samples are referred to as ‘patterned’ *c*-films.

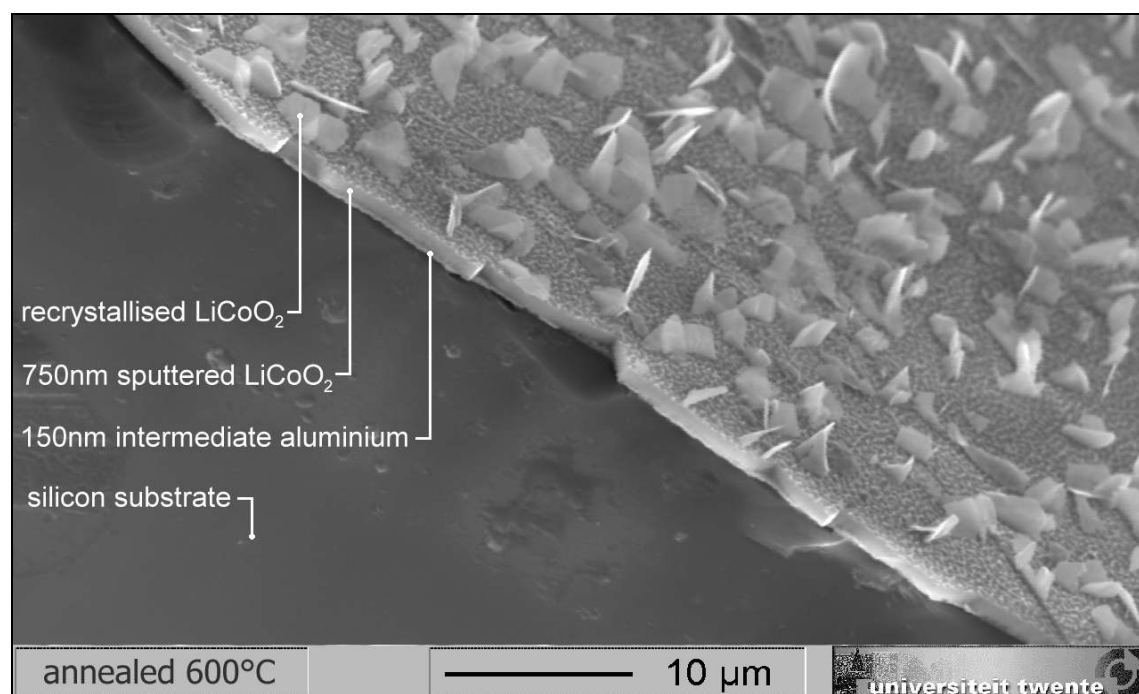


Figure 2: SEM micrograph showing the cross section of a 0.75 μm LiCoO_2 RF-film on silicon substrate having endured prolonged annealing for 180 min at 600°C.

RESULTS

Figure 1 shows the XRD patterns of typical *a*-films and *c*-films deposited on silicon substrates using RF-sputtering and PLD, respectively. Few peaks are observed due to the sharp preferential film orientation. Note that with standard XRD measurement, diffraction is only detected from the lattice planes which are parallel to the substrate surface. The LiCoO_2 crystal structure has been identified using texture plots (not shown here) (1). The inset picture shows both extreme unit cell orientations.

The preferential orientation of the RF-deposited *a*-film is unaffected by film thickness. The film already shows some ordered structure upon deposition, which appears as broad diffractions around the expected (110) peak location. Crystallisation occurs at temperatures above 400°C . The peak width at half maximum (FWHM) in the XRD plot decreases little after annealing 30 min at 600°C (2). Prolonged exposure to elevated temperatures leads to loss of volatile Li_2O and random crystal growth, decreasing the degree of preferential orientation. The SEM micrograph in Figure 2 shows such crystals protruding from the surface of a $0.75\ \mu\text{m}$ LiCoO_2 RF-film annealed 3 hours at 600°C .

The films deposited with PLD generally exhibit a *c*-axis orientation after standard annealing treatment. Substrate heating during deposition only increased the average grain size of the PLD-films significantly. With increasing film thickness ($>0.5\ \mu\text{m}$) the structure becomes more randomly oriented and more diffraction peaks appear in the XRD pattern.

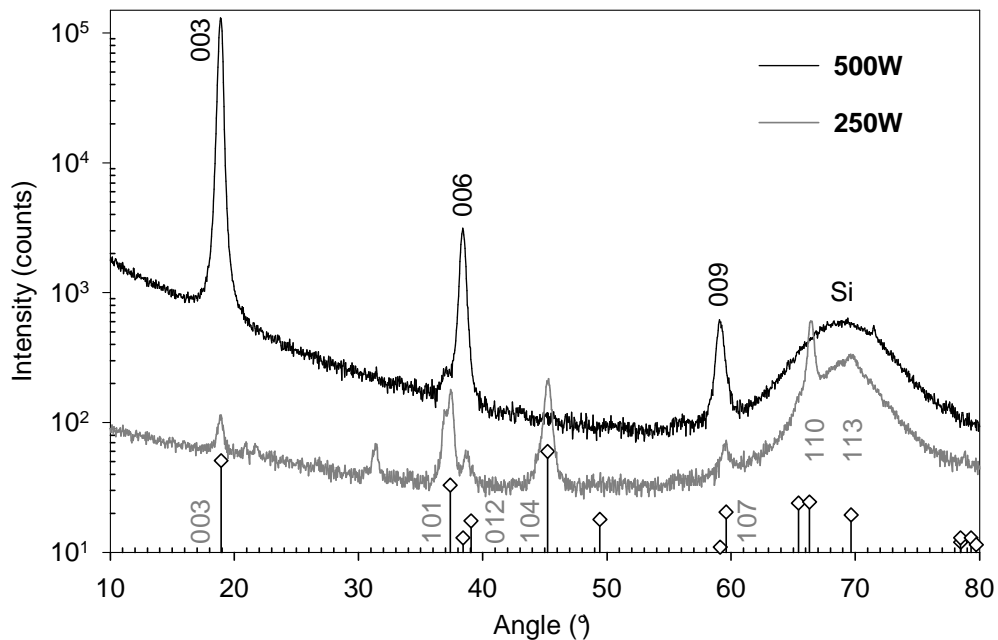


Figure 3: The XRD patterns of two annealed RF-films show a change in preferential orientation towards (104) and even (00 l) with increasing deposition rate. Bars indicate the peak positions and intensities of the LiCoO_2 powder diffraction pattern.

In a separate experiment, PLD has been used to grow a LiCoO_2 film on a $0.1 \mu\text{m}$ a -film seed layer, deposited previously using RF-sputtering (annealed at 600°C , 30 min). A simultaneously deposited (blank silicon) reference sample shows the typical c -film diffraction pattern as plotted in Figure 1 and thus exhibits $(00l)$ lattice plane orientation. However, the PLD-film deposited on the seed layer, which before the deposition experiment showed only the (110) reflection, now shows distinct (006) and (0012) reflections. The typical $(00l)$ orientation is present, but the (003) and (009) reflections are completely absent. Attempts to produce a -films using PLD have been unsuccessful.

The preferential orientation of the RF-deposited films is influenced by the deposition rate, i.e. RF input power density. The XRD plot in Figure 3 shows that with an increase in deposition rate to 250 W RF power (4" target), the (104) diffraction peak has the highest intensity. Deposition with 500W RF-power results in c -films, similar to those produced with PLD. When simultaneous back-sputtering is applied during deposition, c -films are produced without the (003) and (009) diffraction peak, as discussed in the previous paragraph.

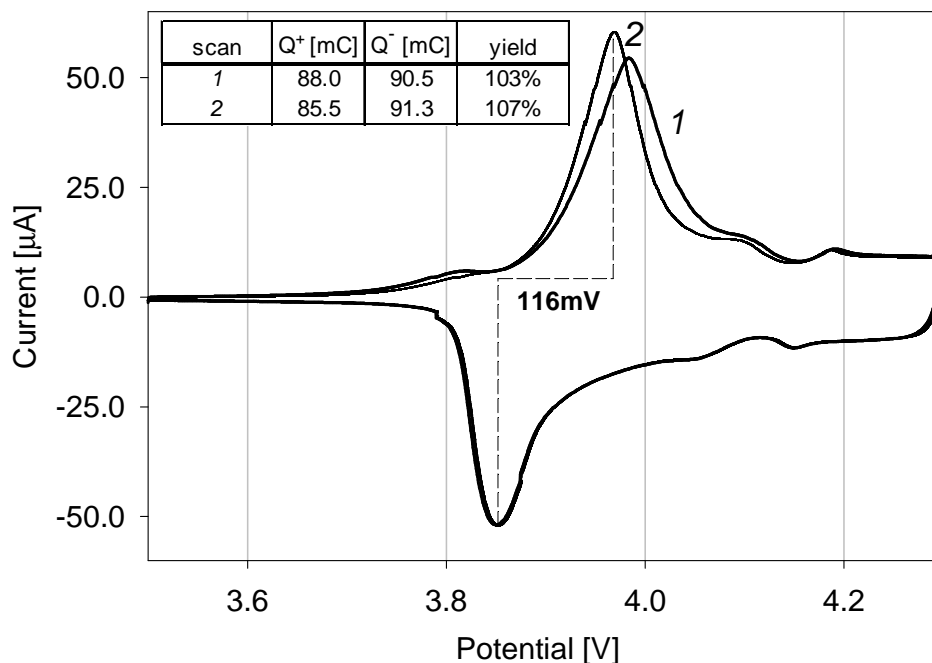


Figure 4: Cyclic voltammogram of $0.5 \mu\text{m}$ a -film on silicon substrate against a metallic lithium counter and reference electrode recorded at a scan rate of $0.1 \text{ mV}\cdot\text{s}^{-1}$.

A cyclic voltammogram of a typical RF-film on silicon substrate is plotted in Figure 4 (scan rate of $0.1 \text{ mV}\cdot\text{s}^{-1}$). The main oxidation and reduction peaks become reproducible after the first cycle and are located at 3.96 V and 3.84 V, respectively. The peak separation between the minor coupled peaks around 4.15 V is close to the theoretical minimum predicted by the Nernst equation. The Faradaic yield of these first cycles is over 100%, which suggests that an increasing amount of electrode material is involved in the intercalation process.

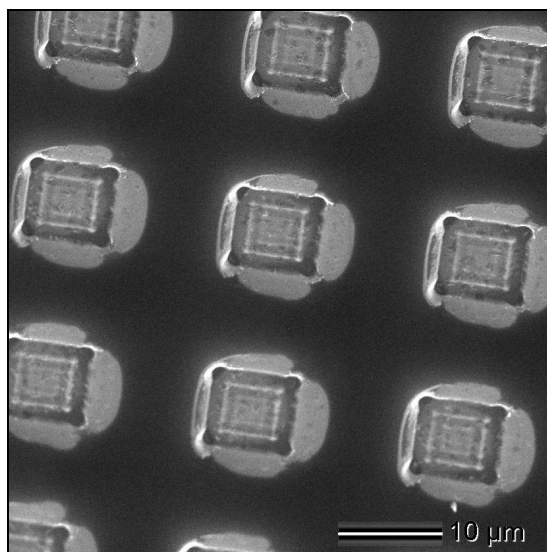


Figure 5: Pattern of square holes etched in a $0.25\ \mu\text{m}$ thick *c*-film on silicon using argon plasma milling.

The *c*-films do not show clear oxidation and reduction features when subjected to cyclic voltammetry at this scan rate. The Faradaic yield remains below 10% and less than 3% of their theoretical capacity is employed. The electrochemical in-activity of these *c*-films makes it difficult to quantify their lithium intercalation behaviour.

The electrochemical performance of the *c*-films on silicon has been improved by introducing pinholes into the LiCoO_2 film (after annealing) through lithography and subsequent wet-chemical etching. Complementary dry-etching experiments with holes as small as $2\ \mu\text{m}$ have also been achieved. However, argon ion milling appears to have a devastating effect on the LiCoO_2 structure at the edges of the pinholes, as visible in Figure 5, and completely diminishes its intercalation activity.

The potential response of an *a*-film on silicon, a regular *c*-film on stainless steel and a ‘patterned’ *c*-film on silicon to pulsed charging is plotted in Figure 6 as a function of time. It was not possible to use a similar pulse for all three samples due to the unequal rate capabilities: the *a*-film is charged with a $50\ \mu\text{A}$ pulses of duration 200 s, followed by a zero-current relaxation period; the stainless steel *c*-film is charged with $10\ \mu\text{A}$ pulses of 150 s; the patterned silicon PLD-film to $2.5\ \mu\text{A}$ pulses of 400 s. The potential relaxation subsequent to a current pulse appears immediate for the *a*-film, while the patterned *c*-film potential relaxation progresses into an exponential decay. The relaxation of the *c*-film deposited on stainless steel is initially also gradual, but it stabilizes after some time at a new equilibrium potential, similar to the *a*-film.

The different potential relaxation behaviour following a current pulse can be attributed to a different apparent diffusion coefficient according to the Galvanostatic Intermittent Titration Technique (GITT), assuming that the intercalation process is diffusion limited. Figure 7 shows the apparent chemical diffusion coefficient of the *a*-film and the patterned *c*-film calculated from the data plotted in Figure 6. The extremely fast ‘recovery’ process

of the *a*-film can be interpreted as a chemical coefficient of 10^{-4} to 10^{-6} $\text{cm}^2.\text{s}^{-1}$, depending on the lithium content. The decreasing rate and capacity of the *a*-film with the number of cycles is due to the formation of a solid-electrolyte interface (SEI) layer, which is detrimental to the intercalation process. The patterned *c*-film exhibits a constant low value of 10^{-13} to 10^{-14} $\text{cm}^2.\text{s}^{-1}$. The potential relaxation data of the patterned *c*-film does not correspond to the GITT model and thus no quantification is allowed. The trend indicates intermediate diffusion kinetics.

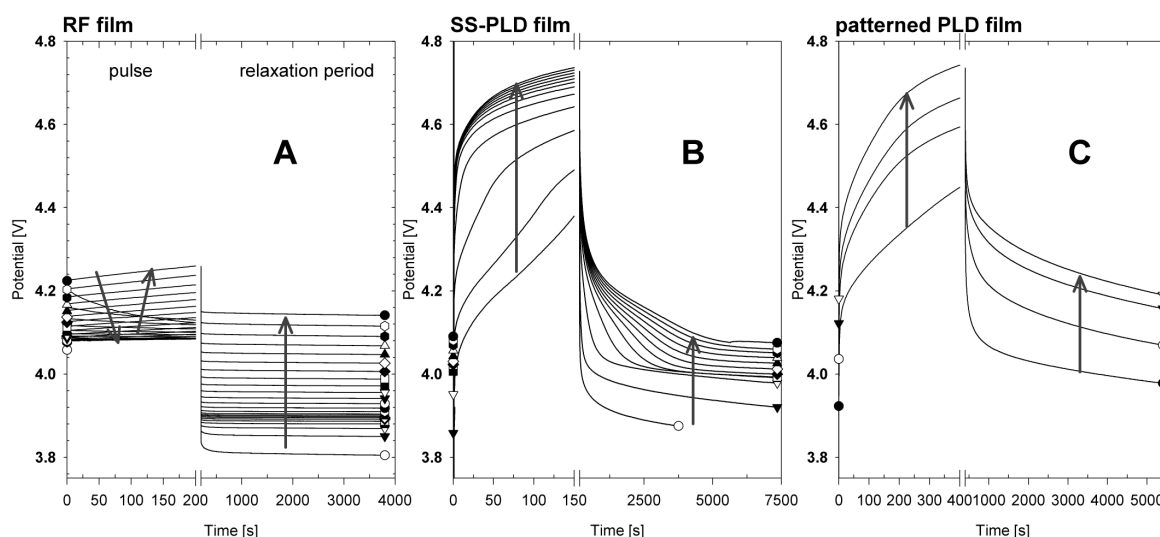


Figure 6: The potential response to sequential charging current pulses of an *a*-film on silicon (**A**: 200 s, 50 μA), a *c*-film on stainless steel (**B**: 150 s, 10 μA) and a patterned *c*-film on silicon (**C**: 400 s, 2.5 μA) plotted as a function of time. During the relaxation period the electrode regains equilibrium.

DISCUSSION

The films deposited with PLD are likely to exhibit a *c*-axis orientation. The (00*l*) planes of LiCoO_2 are hexagonally close-packed and have the highest density and a low surface energy. At high deposition rates these planes are formed parallel to the substrate surface to cope with the high material flux (6). PLD is based on short plasma bursts for deposition and exhibits high momentary film growth rates. The preferential *c*-axis orientation of the PLD-films becomes random with increasing film thickness (>0.25 μm), as the physical alignment process is no longer uniform with increasing surface roughness. Thus, the *c*-films on stainless steel substrates are **not** as preferentially oriented as those on silicon substrates.

The RF-films are actually grown at low deposition rate. LiCoO_2 crystal growth occurs fastest along the *a*-axis towards the source of the material flux. As this direction is oriented normal to the substrate, stable '*a*-films' are produced independent of film thickness. At intermediate RF-deposition rates a tilted (104) orientation is observed and at high rates the previously discussed *c*-axis orientation re-appears. During annealing

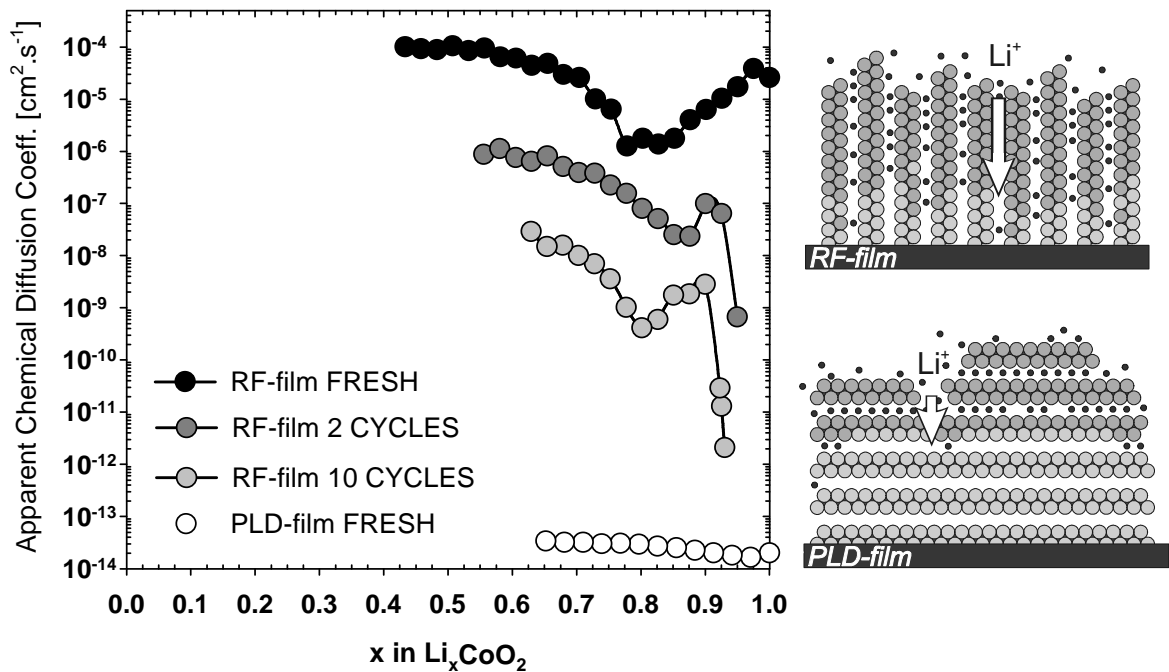


Figure 7: The Apparent Chemical Diffusion Coefficient as determined for the *a*- and *c*-films from GITT-measurements as a function of x . The inset picture shows the preferential orientation of the lithium diffusion plane for both films.

treatment at 600°C further crystallisation occurs and the film develops a columnar, polycrystalline structure. Long exposure to elevated temperatures results in outgrowth of crystals from the film surface, as visible in Figure 2.

The preferential orientation is not influenced by the substrate material; there is no indication of epitaxial growth. For example, the PLD-film deposited on an *a*-film seed layer does not adopt the existing (110) orientation, but exhibits the usual (00 l) orientation. However, the absence of the (003) and (009) diffraction peak indicates a true rocksalt (NaCl) crystal structure exists due to cationic disorder (7). The random distribution of the lithium and cobalt ions also removes the internal lithium diffusion pathways. Hence, the rocksalt films show no intercalation activity.

In case of thin-film LiCoO₂ electrodes, the lithium diffusion plane and its orientation towards the electrolyte solution primarily determine its electrochemical intercalation behaviour. The two contrasting situations are visualised in the inset of Figure 7. Lithium (de-)intercalation in an *a*-film proceeds parallel to the two-dimensional lithium diffusion plane, while in case of the PLD-film the overall intercalation direction is normal to these diffusion planes. The apparent chemical diffusion coefficient plotted in Figure 7 indicates that the lithium diffusion within these planes is extremely fast and transport of lithium across the CoO₂ sandwiches is negligible. Hence, the intercalation capability of a *c*-film is highly dependent on other means of inward lithium transport (e.g. grain boundaries, defects, cracks). This hints to be the second advantage of using rough substrates.

The number of pinholes of the *c*-film on silicon substrates can accurately be increased using lithographic patterning. The *a*-film shows no gain from patterning, since the favourable host alignment already provides optimal exposure to the electrolyte solution. Wet-etch patterning of a *c*-film reduces the overpotential observed during constant current cycling (not shown) and increases the current rate capability to 25 μA . Generally, the reversible capacity of the *c*-films increases with patterning from 3% to 15% of its theoretical capacity. Note however, that the mesh of the gauze-like pattern remains large compared to the film thickness. Apparently not all the active material is 'accessible' from the electrolyte solution and is thus incapable of intercalation.

The microscopically rough surfaces of the polished stainless steel substrates are expected to introduce numerous defects in the deposited film. It is suggested that the high degree of defects in the *c*-film on stainless steel increases the diffusion plane exposure and decreases the lithium diffusion distance within the intercalation host. Thus, relatively fast equilibration of the intercalated lithium concentration profile is achieved. This coincides with the superior electrochemical behaviour observed for stainless steel PLD-films compared to the regular and even the patterned *c*-films on silicon substrates. In Figure 5 the current pulse response of the stainless steel *c*-film appears to be combination of the *a*-film and the patterned *c*-film on silicon. The high overpotential during the pulse and the slow potential relaxation afterwards is typical for *c*-films, which is a result of the limited intercalation rate connected to the slow internal lithium diffusion. On the other hand, the stable potential obtained after a specific relaxation period is common for *a*-films. A similar effect could probably be achieved for the patterned *c*-films on silicon, if gauze-like patterns of sub-micrometer mesh dimensions could be etched in its surface.

The lithium intercalation capability of thin-film LiCoO_2 electrodes depends heavily on the orientation of the two-dimensional diffusion plane toward the electrolyte solution. Pinholes and film defects may compensate an unfavourable (001) host orientation, but only to a certain degree. The *a*-films are the most promising electrodes for application in solid state devices and are currently being tested in high power micro-batteries.

CONCLUSIONS

The alignment of the two-dimensional diffusion plane to the electrolyte solution appears perpendicular (hence accessible) or parallel (thus inaccessible) in *a*-films and *c*-films, respectively and is related to the rate of deposition. The large influence of the host orientation on the intercalation process is reflected by the electrochemical behaviour. The *a*-films utilise almost their full theoretical capacity during cycling at high current densities showing low overpotentials. This is in contrast with the *c*-films, which show inferior reversible capacity at low current densities together with extreme overpotentials. In the latter case the electrochemical properties may be improved by introducing defects in the thin-film electrode. This is either achieved in an uncontrolled manner through deposition on stainless steel substrates or accurately using lithographic patterning techniques. Still, the increased exposure of the diffusion plane through defect introduction cannot compensate for the adverse effect of its unfavourable alignment. The

preparation of LiCoO₂ thin-film electrodes in the preferential (110) orientation (RF-sputtering) is recommended for superior electrochemical intercalation performance.

ACKNOWLEDGEMENT

This research was made possible due to financial support from FOM. The authors are indebted to Philips Research Laboratory for technical support on sample preparation and characterization. Special thanks are due to J.F.M. Cillessen for operation and assistance on the PLD equipment, H. Koster for the SEM analysis; the Philips CFT department for the XRD measurements.

REFERENCES

1. P.J. Bouwman, B.A. Boukamp, H.J.M. Bouwmeester, H.J. Wondergem, P.H.L. Notten, *J. Electrochem. Soc.*, **148** A311 (2001).
2. P.J. Bouwman, B.A. Boukamp, H.J.M. Bouwmeester, P.H.L. Notten, *J. Electrochem. Soc.*, **149** A699 (2002).
3. P. Fragnaud, T. Brousse, D.M. Schleich, *J. of Power Sources*, **63**, 187-91 (1996).
4. K.A. Striebel, C.Z. Deng, S.J. Wen, E.J. Cairns, *J. Electrochem. Soc.*, **143** 1821 (1996).
5. Y. Iriyama, M. Inaba, T. Abe, Z. Ogumi, *J. of Power Sources*, **94** 175 (2001).
6. K. Nishioka, N. Mizutani, H. Komiyama, *J. Electrochem. Soc.*, **147** 1440 (2000).
7. H.W. Wang, Y.I. Jang, B. Huang, D.R. Sadoway, Y.M. Chiang, *J. Electrochem. Soc.*, **146**, 473 (1999).